

the periphery of the cell. After the exchange of AMP against ATP and of calcium-free calmodulin against calcium-loaded calmodulin the ATPase complex is workable again.

Obviously, the energy transfer via calcium has the advantage that in case of emergency needs great amounts of free energy can be made available in a short time independently of the ATP supply. This is done by flushing calcium-free calmodulin produced by continuous pumping and stored in the nearly calcium-free cytosol with calcium coming from the periphery or any other calcium source of the cell. Thus the calcium/calmodulin system is part of a storage power station of the cell.

In the pumping process based on the calcium transfer by calmodulin the lowest calcium concentration is set by the spontaneous dissociation of the calcium/calmodulin complex. This is consistent with the assumption made above

to evaluate the upper limit of the free energy production by the calcium-loading of calmodulin.

If a sustained stimulation results in a sustained reaction of the cell, the detour, via the cytosol, in the transport of calcium-loaded and calcium-free calmodulin between the adenylate cyclase complex and the ATPase complex may be avoided. So the calcium cycling in the membrane region, described in [4] will be established.

An increase in the concentration of calcium-loaded calmodulin in the cytosol not only starts the pumping process mentioned above but also activates phosphodiesterase which, as is well known, destroys cAMP by hydrolysis [2].

The main difference in the new concept as compared to the former models is seen in the fact that it attributes to calcium not only the function of a messenger but also the function of a trans-

porter for the free energy needed to start endergonic reactions. The transfer of free energy by calcium does not need to be restricted to the production of cAMP for the initiation of chemical reactions. It can be expected that also for other endergonic processes in the cell, e.g., for the generation of mechanical work the transfer of free energy by calcium is of importance.

Received January 9, 1990

1. Sutherland, E. W.: *Angew. Chem.* 84, 1117 (1972)
2. Cheung, W. Y.: *Sci. Am.* 246, 48 (1982)
3. Carafoli, E., Penniston, J. T.: *ibid.* 253, 50 (1985)
4. Alkon, D. L., Rasmussen, H.: *Science* 239, 998 (1988)
5. Stryer, L.: *Biochemistry*, p. 810. San Francisco: Freeman 1975

Naturwissenschaften 77, 177 – 179 (1990) © Springer-Verlag 1990

Activated State in the Lepidocrocite Structure During Thermal Treatment

A. U. Gehring

Institute of Water Resources and Water Pollution Control (EAWAG),
Swiss Federal Institute of Technology (ETH), Zürich, CH-8600 Dübendorf

R. Karthein

Laboratorium für Physikalische Chemie der ETH, CH-8092 Zürich

A. Reller

Institute for Inorganic Chemistry, University of Zürich, CH-8057 Zürich

In natural environments such as soils and sedimentary iron ores ferric(oxy)hydroxides are major components [1, 2]. Upon heating to approximately 500–700 K, e.g., during forest and bush burning or metamorphic processes, these compounds convert to ferric oxides. The structural and morphological changes during the conversion have been considered in the literature [3, 4]. The reaction mechanism on an atomic level as a function of temperature, which gives insight into

thermal conversion processes in natural environments, has not been reported yet. The transformation of lepidocrocite (γ -FeOOH), a ferric(oxy)hydroxide often found in soils, to the ferric oxide maghemite (γ -Fe₂O₃) during thermal treatment is examined in this study.

The orange colored lepidocrocite under investigation was synthesized by oxidation of a 0.5 M FeCl₂ solution (Merck p.a.) with NaNO₂ after the method described in [5]. The precipitate was

washed from the electrolytes with bidistilled water, stored at about pH 7 for 90 days, then filtered and dried in an oven at 313 K.

The synthetic lepidocrocite was identified by XRD. The thermal behavior was investigated by differential scanning calorimetry and thermogravimetry (DSC/TG). The course of the thermogravimetric measurements shows a well-defined change of weight due to loss of stoichiometric H₂O between 470 and 520 K. This dehydration process appears in DSC as a maximum endothermal effect indicating the conversion of lepidocrocite into maghemite. In addition to this endothermal peak, a broad exothermal peak is observed between 400 and 450 K.

In order to find structural and morphological evidence for this exothermal process, high-resolution electron microscopy (HRTEM) and electron diffraction were carried out. Under the HRTEM lepidocrocite shows lath-shaped idiomorphous crystallites (Fig. 1a). The electron diffraction pattern of the crystallites reveals the presence of crystalline particles (Fig. 1b). Under prolonged irradiation by the electron beam the lath-shaped lepidocrocite can

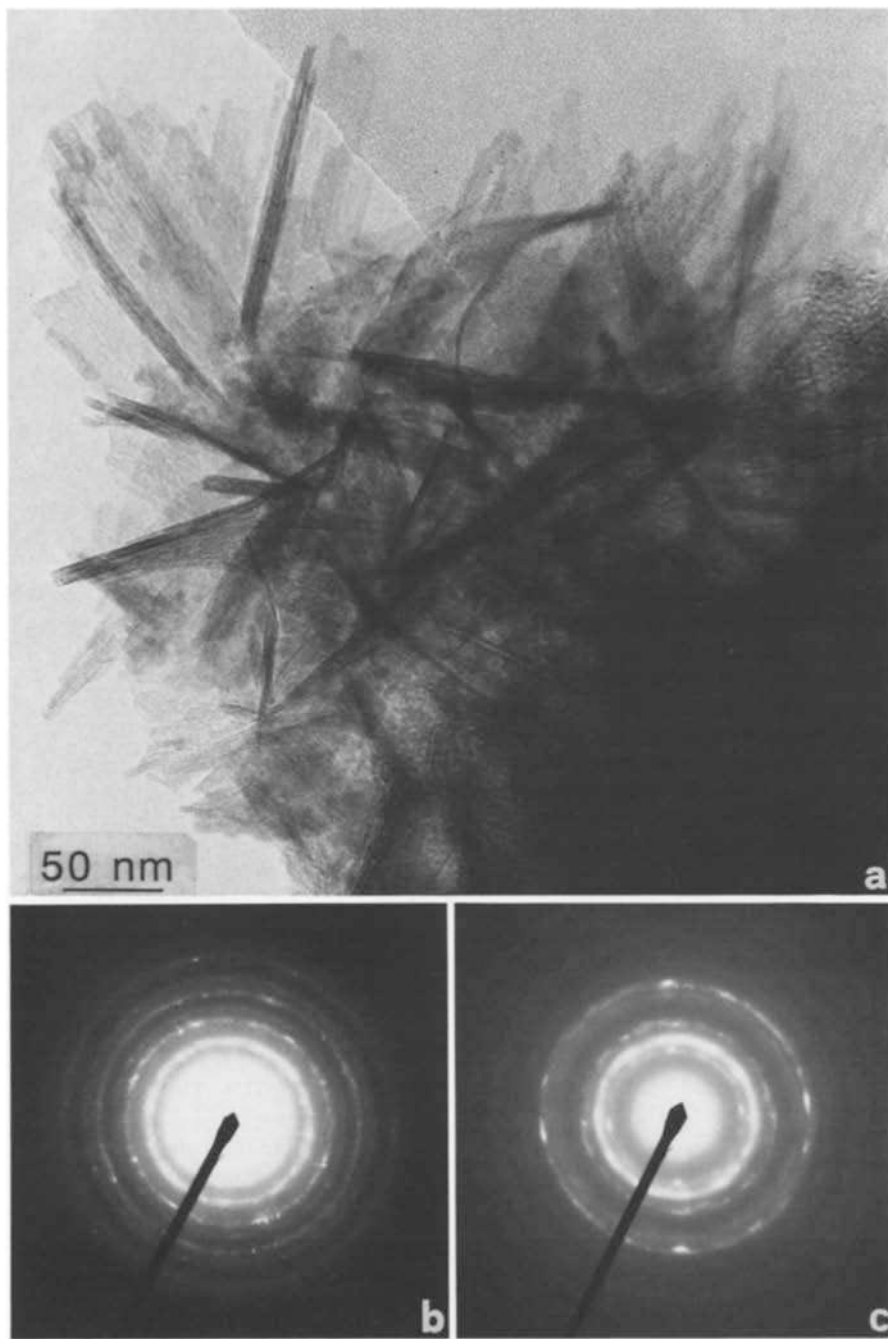


Fig. 1. a) Electron micrograph of lepidocrocite crystallites with lath-shaped morphology. b) Corresponding electron diffraction pattern providing the lepidocrocite structure. c) Electron diffraction pattern of maghemite obtained by prolonged irradiation of lepidocrocite crystallites

be transformed into pseudomorphous maghemite (Fig. 1c). This conversion indicates a rearrangement of the lepidocrocite structure on a microcrystalline level. Furthermore, this finding suggests that the lepidocrocite is highly activated before the actual dehydration

takes place. This activated state can be attributed to the exothermal peak found by DSC between 400 and 450 K. Since this exothermal process is not caused by fundamental morphological changes nor by significant weight loss, i.e., compositional changes, the

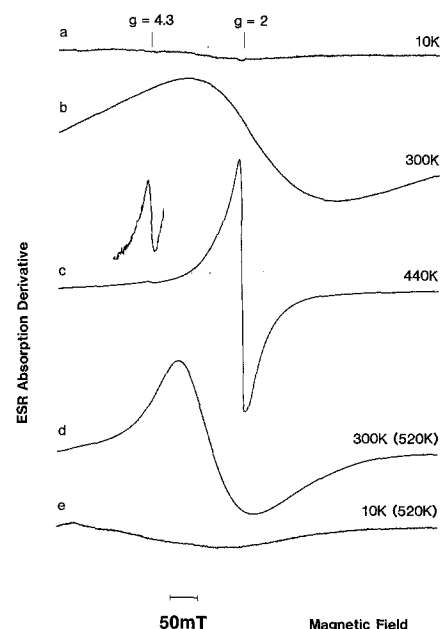


Fig. 2. ESR spectra of a lepidocrocite sample measured at a) 10 K, b) 300 K. Spectrum c) was taken of a lepidocrocite sample heated at 440 K for 0.5 h, measured at this temperature and gain-reduced by a factor of 0.1. In addition, the $g = 4.3$ signal is displayed on the same scale as the above spectra. In d) and e) the lepidocrocite sample was heated to 520 K, annealed for 0.5 h and then measured at 300 and 10 K, respectively. Spectrum d) is gain-reduced by a factor of 0.01

structural rearrangements within the lepidocrocite have to take place on an atomic level.

Electron spin resonance (ESR) spectra have been recorded at X-band using 100-kHz field modulation during the conversion of lepidocrocite into maghemite. At room temperature (RT) lepidocrocite is paramagnetic and shows a broad ESR signal with a line width of 250 mT and a zero-crossing near a g -value of 2 (Fig. 2b). This broad line width is mainly caused by the electron spin-spin interaction between the Fe^{3+} ions within the [001] layers made up of edge-sharing FeO_6 octahedra [6], and by the particle size and morphology of the lepidocrocite [7]. Magnetic ordering in the lepidocrocite beginning below the Néel temperature leads to a drastic decrease of the ESR signal intensity and at 10 K the signal disappears (Fig. 2a). Upon heating of the lepidocrocite in the ESR cavity two narrow signals evolve simultaneously at 410 K, a strong peak at $g = 2$ and a

weak one at $g=4.3$. Low-temperature measurements before heating (Fig. 2a) exclude that the broad lepidocrocite spectrum masks the weaker $g=4.3$ signal. With increasing temperature, however, both narrow signals become more pronounced (Fig. 2c). These new signals superimpose the lepidocrocite signal found at RT and dominate the ESR spectrum. After heating to 520 K the strong peak shifts slightly from $g=2$ to about $g=2.5$. Furthermore, the line width broadens to 140 mT and the intensity of the signal increases significantly (Fig. 2d). When cooling down to 10 K the intensity decreases and only a very weak signal can be measured (Fig. 2e). The occurrence of the $g=2$ signal above 410 K can be interpreted as a consequence of maghemite formation and therefore of the beginning conversion process. The correlation with HRTEM observations suggests that this signal can be attributed to pseudomorphic maghemite. The strong increase of the ESR signal at $g=2$ above 410 K indicates the disintegration of the lepidocrocite structure before the main evolution of water detected by TG occurs. The onset of this process explains the broad exothermal peak found by DSC. At 520 K where the maximum endothermic effect is observed, the resonance field changes only little, but a drastic increase in the line width and a maximum intensity of the ESR signal are detected. It is well established that the magnetic properties of ferric oxides are dependent on the crystallinity [8]. Furthermore, the ESR line shape can be strongly influenced by the domain structure of the ferric oxides [9]. There-

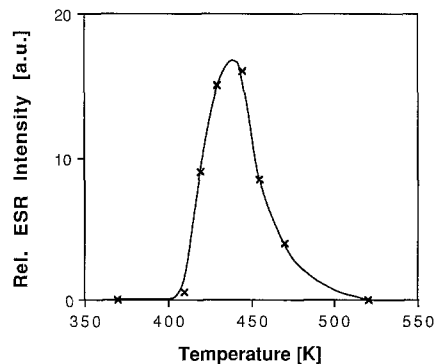


Fig. 3. Temperature vs. relative intensity in arbitrary units of the ESR signal at $g=4.3$

fore, it is very likely that the observed change in the $g=2$ ESR signal is mainly caused by the growth of ferrimagnetic maghemite crystallites during the thermal treatment.

The $g=4.3$ signal is characteristic for Fe^{3+} ions in distorted coordination polyhedra of rhombic symmetry [10]. The occurrence of this signal at 410 K indicates a rearrangement within the lepidocrocite structure on an atomic level. The temperature dependence of the $g=4.3$ signal reveals a maximum intensity at 450 K and a subsequent drop to zero at 520 K (Fig. 3). This suggests that the structural reaction refers to an intermediate change of the Fe^{3+} coordination before the actual evolution of water, i.e., the condensation of water molecules. Regarding the lepidocrocite crystal structure with hydrogen interlinking the [001] layers [6] and the conversion mechanism leading to the condensation of water molecules, the $g=4.3$ signal is explained as an enhanced distortion of FeO_6 octahedra

due to the dynamic rearrangement of the positions of the oxygen and hydrogen atoms.

This result leads to the conclusion that ESR spectroscopy defines and characterizes an intermediate activated state of the lepidocrocite structure prior to the actual formation of crystalline maghemite.

The authors would like to thank G. Bondietti (EAWAG) for providing the lepidocrocite sample. This project was supported by the Swiss National Foundation project No. 2.942-0.88 and a grant of the Board of the Swiss Federal Institute of Technology.

Received October 23, 1989 and February 5, 1990

- Schwertmann, U., in: *Iron in Soils and Clay Minerals*, p. 267 (Stucki, J. W., et al., eds.). Dordrecht: Reidel 1989
- Gehring, A. U.: *Geol. Soc. Spec. Publ.* 46, 133 (1989)
- Gómez-Villacieros, R., Hernán, L., Morales, J., Tirado, J. L.: *J. Coll. Interf. Sci.* 101, 392 (1984)
- Hedley, I. G.: *Phys. Earth Planet. Inter.* 1, 103 (1968)
- Glemser, O.: *Ber. dtsh. chem. Ges.* 71, 158 (1938)
- Christensen, H., Christensen, A. N.: *Acta Chem. Scand.* A32, 87 (1978)
- Kraan, A. M. van der: *Phys. stat. sol. a* 18, 216 (1973)
- Murad, E., Schwertmann, U.: *Miner. Mag.* 48, 507 (1984)
- Griscom, D. L.: *J. Non-Cryst. Solids* 68, 81 (1984)
- Calas, G.: *Rev. Miner.* 18, 513 (1988)

Änderungen der Serumparameter eines amphibisch lebenden Wirbeltieres

Bioindikormodell zum Nachweis von Strahlenbelastung

M. Giannetti, H. Strick, A. Trux und W. J. Kloft

Institut für Angewandte Zoologie der Universität, D-5300 Bonn

Bei der kontinuierlichen Zunahme einer anthropogenen Strahlenexposition der Ökosphäre durch steigende Nutzung von Kernspaltungen für friedliche und militärische Zwecke kommt der Ab-

schätzung des Strahlenrisikos besondere Bedeutung zu [1]. Biologische Indikatoren für radioaktive Kontaminationen von Ökosystemen können physikalischen oder chemischen Detek-

tionsverfahren überlegen sein, wenn sie Belastungen auch im niederen Dosisbereich (mit sensiblen physiologischen Parametern) und auch noch lange Zeit nach der Strahlenbelastung (u.U. mit vererbaren Parametern) anzeigen.

Aufbauend auf den Arbeiten von Strick et al. [2, 3] wird ein Zeigermodell entwickelt, das diesen Anforderungen genügt: Der Indikatororganismus muß schnell, irreversibel, reproduzierbar, signifikant und im Idealfall auch noch durch Weitergabe an Nachkommen auf eine Noxe reagieren.

Als Zeigerorganismus wurde der mit ^{45}Ca behandelte Südafrikanische Kral-